On the Crystal Structure of Azafullerene ($(C_{59}N)_2$)

C. M. Brown,[†] L. Cristofolini,[†] K. Kordatos,[†]
K. Prassides,*[,†] C. Bellavia,[‡] R. González,[‡]
M. Keshavarz-K.,[‡] F. Wudl,*[,‡] A. K. Cheetham,*[,‡]
J. P. Zhang,[‡] W. Andreoni,[§] A. Curioni,[§,⊥]
A. N. Fitch,[||] and P. Pattison[#]

School of Chemistry and Molecular Sciences
University of Sussex, Brighton BN1 9QJ, UK
Institute for Polymers and Organic Solids and
Materials Research Laboratory, University of
California, Santa Barbara, California 93106
IBM Research Division, Zurich Research Laboratory
8803 Rüschlikon, Switzerland; Scuola Normale
Superiore, Piazza dei Cavalieri 7, 56126 Pisa, Italy
European Synchrotron Radiation Facility, B.P. 220
F-38043 Grenoble, France, and Université de
Lausanne, Institut de Cristallographie
CH-1015 Lausanne, Switzerland

Received July 3, 1996

The crystal structure of solid C_{60} can be understood to a good approximation using simple crystal structure arguments, based on the close packing of spheroidal molecules. The simplest variant of C_{60} that can be envisaged consists of substituting one of the carbon atoms of the fullerene skeleton by an aliovalent atom to afford a $C_{59}A$ molecule. Indeed modification of C_{60} by rational organic synthesis recently led to the first successful incorporation of a heteroatom (nitrogen) in the fullerene framework and isolation and characterization in the bulk of such a heterofullerene.[1] However, as a result of the trivalency of nitrogen, compared to the tetravalency of carbon, the neutral azafullerene molecule is open shell and as such is found to rapidly dimerize yielding $(C_{59}N)_2$. Reaction with excess alkali metals[2] leads to the breaking of the bridging C−C bond and the dimer reverts to the monomeric azafulleride ion, $(C_{59}N)^{6-}$, thereby displaying an intercalation chemistry analogous to that of C_{60}. The as-prepared azafullerene solid shows a remarkable tendency to self-assemble into large hollow spheroidal particles.[3] In addition, high-pressure diffraction measurements reveal an anisotropic solid with a somewhat smaller compressibility,[4] $\kappa = 0.05$ GPa^{-1}, than that of pristine C_{60}.

Here we present the results of a synchrotron X-ray powder diffraction study of the structure of sublimed $(C_{59}N)_2$. The pattern reveals the presence of a superlattice stemming from the molecular dimerization. Short intradimer center-to-center ball distances of 9.41 Å are present, considerably shorter than the average distance to the 11 other nearest neighbors of 9.97 Å (cf. nearest neighbor center-to-center distance in cubic C_{60} is 10.02 Å). Recent density functional theory-based optimization of the molecular structure of $(C_{59}N)_2$ reveals a gain in energy upon dimerization[5] and is consistent with the above intradimer distance; at the same time, it also reveals sizeable structural changes in the vicinity of the bridges. The optimized dimer structure was introduced in the crystal structure refinements, allowing us to obtain additional information on intermolecular interactions and orientational disorder.

The azafullerene sample used in the present study was prepared from a "holey bucky" as described previously[1] and was purified by HPLC on a Cosmosil "Buckyprep" column using toluene as eluent. Solid $(C_{59}N)_2$ was obtained from a solution in *o*-dichlorobenzene (ODCB), which was evaporated rapidly to dryness in a rotary evaporator and then recrystallized from a CS_2 solution. The sample was subsequently sublimed under dynamic vacuum (∼10^{-6} Torr) at 500 °C for 12 h. High-resolution synchrotron X-ray diffraction measurements ($\lambda = 0.8717$ Å, $2\theta = 2-40°$) on the sample sealed in a thin-wall glass capillary 0.5 mm in diameter were performed at 278 and 500 K at the SRS Station 9.1, Daresbury Laboratory, U.K. Images of the Debye−Scherrer rings from the same sample were also recorded at 295 K on the Mar Research circular image plate system (diameter = 300 mm) on line A of the Swiss-Norwegian beamline (SNBL) at the European Synchrotron Radiation Facility, Grenoble ($\lambda = 0.8736$ Å). One-dimensional diffraction patterns were obtained by integrating around the rings using a local software (program FIT2D). Data analysis was performed with the PROFIL[6] suite of Rietveld analysis programs, incorporating form factors for spherically disordered molecules and the LeBail pattern decomposition technique.[7]

Inspection of the XRD profile (shown as dots in Figure 1) reveals essentially no Bragg peaks above $2\theta_{max} \sim 20°$ ($Q_{max} \sim 2.5$ Å^{-1}) at all temperatures. Most of the intensity is concentrated in a cluster of diffraction peaks at $2\theta \sim 6°$, 10°, and 12°, where the dominant peaks of a pseudo-cubic solid with lattice dimensions of the same order as C_{60} are expected to lie. The instrumental resolution allows for splittings to be observed, signifying a reduced crystal symmetry. One unusual feature is the observation of a significant peak on the leading edge of the $(111)_{cubic}$ reflection at ∼6°; we ascribe this to the presence of hexagonal stacking faults in the fcc parent structure, an interpretation that is confirmed by selected area electron diffraction patterns. More important, however, is the observation of a superlattice peak at ∼3° that indexes as $(^1/_2,^1/_2,^1/_2)_{cubic}$ in the fundamental

---

[†] University of Sussex.

[‡] University of California, Santa Barbara.

[§] IBM Zurich.

[⊥] Scuola Normale Pisa.

[||] ESRF Grenoble.

[#] Université de Lausanne.

* To whom correspondence should be addressed.

(1) Hummelen, J. C.; Knight, B.; Pavlovich, J.; González, R.; Wudl, F. *Science* **1995**, *269*, 1554. Hummelen, J. C.; Prato, M.; Wudl, F. *J. Am. Chem. Soc.* **1995**, *117*, 7003.

(2) Prassides, K.; Keshavarz-K., M.; Hummelen, J. C.; Andreoni, W.; Giannozzi, P.; Beer, E.; Bellavia, C.; Cristofolini, L.; González, R.; Lappas, A.; Murata, Y.; Malecki, M.; Srdanov, V.; Wudl, F. *Science* **1996**, *271*, 1833.

(3) Prassides, K.; Keshavarz-K., M.; Beer, E.; Bellavia, C.; González, R.; Murata, Y.; Wudl, F.; Cheetham, A. K.; Zhang, J. P. *Chem. Mater.* **1996**, *8*, 2405.

(4) Brown, C. M.; Beer, E.; Bellavia, C.; Cristofolini, L.; González, R.; Hanfland, M.; Häusermann, D.; Keshavarz-K., M.; Kordatos, K.; Prassides, K.; Wudl, F. *J. Am. Chem. Soc.* **1996**, *118*, 8715.

(5) Andreoni, W.; Curioni, A.; Holczer, K.; Prassides, K.; Keshavarz-K., M.; Hummelen, J. C.; Wudl, F. *J. Am. Chem. Soc.*, in press. Calculations are performed using the Becke−Lee−Yang−Parr approximation for the exchange functionals (Becke, A. D. *Phys. Rev. A* **1988**, *38*, 3098. Lee, C.; Yang, W.; Parr, R. G. *Phys. Rev. B* **1988**, *37*, 785).

(6) Cockcroft, J. K. *Program PROFIL*; Birkbeck College, London, U.K., 1994.

(7) LeBail, A.; Duroy, H.; Fourquet, J. L. *Mater. Res. Bull.* **1988**, *23*, 447.

S0897-4756(96)00354-7 CCC: $12.00

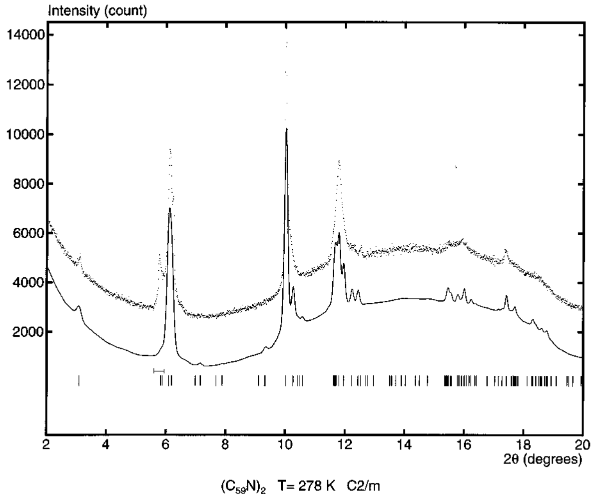

Figure 1. Measured synchrotron X-ray powder diffraction pattern (points) of $(C_{59}N)_2$ in the range 2−20° at 278 K (λ = 0.8717 Å). The profile calculated using a monoclinic cell with symmetry *C*2/*m* and employing two merohedral images of the $(C_{59}N)_2$ dimers rotated by 1.5° about the *c* axis of the unit cell is also shown and is displaced downward for clarity (solid line). Vertical marks indicate the position of the Bragg reflections for the *C*2/*m* monoclinic cell.

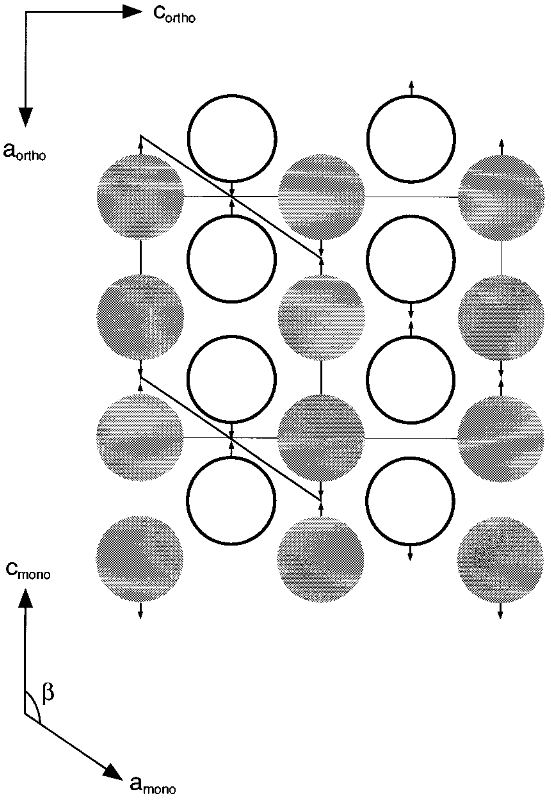

Figure 2. Schematic representation of the structure of $(C_{59}N)_2$ showing the relationship between the orthorhombic and monoclinic unit cells described in the text.

pseudo-cubic cell with lattice dimensions $a_0 \sim 14.1$ Å. This necessitates the existence of an enlarged unit cell doubled along all three dimensions $(2a_0,2a_0,2a_0)$ or (Figure 2) a body-centered orthorhombic cell with dimensions $(\sqrt{2}a_0,1/\sqrt{2}a_0,2a_0)$ whence the observed superlattice peak indexes as $(101)_{\mathrm{orthorhombic}}$. Unit-cell parameters for the latter cell were extracted with the LeBail pattern decomposition technique by employing the *Bmmm* space group, giving a = 19.44 Å, b = 9.96 Å, and c = 28.49 Å at 278 K.

Table 1. Structural Data for Solid $(C_{59}N)_2$ at Different Temperatures (Space Group *C*2/*m*)

T (K)	diffractometer	*a* (Å)	*b* (Å)	*c* (Å)	β (°)
500	9.1 (SRS)	17.312(6)	9.998(2)	19.524(8)	124.33(2)
295	SNBL (ESRF)	17.258(5)	9.968(3)	19.459(4)	124.32(2)
278	9.1 (SRS)	17.250(7)	9.959(3)	19.445(8)	124.31(2)

A strict constraint imposed by the observation of finite intensity for the $(101)_{\mathrm{orthorhombic}}$ superlattice peak is that the $C_{59}N$ molecular units can no longer occupy the high-symmetry ideal positions in the unit cell, thus precluding an undistorted monomeric structure as this will result in negligible intensity at the $(101)_{\mathrm{orthorhombic}}$ position. We therefore explored in detail the possibility of relaxing the molecular positions by allowing adjacent molecules, considered in the first instance as quasi-spherical units of radius 3.55 Å, to move toward each other. Under such circumstances, however, an orthorhombic crystal symmetry is not possible and in the case of orientationally disordered $C_{59}N$ units it reduces to monoclinic with lattice dimensions a = 17.25 Å, b = 9.96 Å, c = 19.44 Å, β = 124.3° at 278 K (space group *C*2/*m*, Figure 2). In this case, if the molecules are allowed to move along the *c* axis only, their optimal position, which reproduces the intensity of the $(101)_{\mathrm{orthorhombic}}$ peak normalized to the intensities of the peaks at ~10° and ~12°, is found to be (0,0,0.242). These positions are consistent with the above-mentioned intradimer center-to-center separations of $(C_{59}N)_2$ units along *c* of 9.41 Å. The other 11 nearest-neighbor distances range between 9.81 and 10.11 Å, resulting in the above-mentioned average of 9.97 Å, only marginally smaller than the 10.02 Å distances in orientationally disordered solid C_{60}. Table 1 collects together the lattice constant information derived from the analysis of the diffraction data at the temperatures studied. No significant anisotropy in the thermal expansivity is observed.

The observation of only a single superlattice peak and the lack of significant intensity in the diffraction profile at high Q severely hinders more detailed analysis, as it is not possible to shift the azafullerene units in the other two directions in an uncorrelated way. However, we note that there exists good agreement between the intradimer separation derived in the present analysis using the spherical approximation for each monomer and that (9.31 Å) obtained from optimization of the molecular structure of $(C_{59}N)_2$ by density-functional calculations.[5] These reveal that the dimer comprises two units linked by one long C−C bond (1.61 Å) with the nitrogen atoms in a trans configuration and that dimerization is accompanied by a gain in energy of ~18 kcal/mol. Hence, we proceeded by replacing the quasi-spherical units employed thus far by the optimized molecular structure, with the principal molecular axis, defined by the centers of the two monomers aligning with the *c* axis. In the general case, the appropriate monoclinic space group is $P2_1/a$. We first explored the effects of orientational order by allowing the dimer to rotate about its principal axis. This affects the calculated intensity of the superlattice peak very little with changes evident only at higher Bragg angles. A detailed comparison between the various orientations gives the best agreement with our data for the two orientational images of the dimer in which the *b*-axis is essentially perpendicular to a hexagon−hexagon (6:6) bond (Figure 3); in this special case, the appropriate monoclinic space

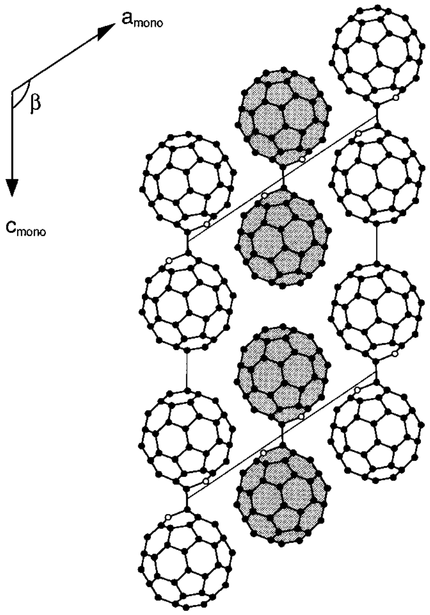

Figure 3. Unit-cell basal plane projection of the structure of $(C_{59}N)_2$ down the *b* monoclinic axis. Only one of the two orientations, related by a 180° rotation about the *c* axis is shown.

group is $C2/m$. Superimposing these two merohedral images is again consistent with $C2/m$, but in the absence of well-resolved data at higher Q, we cannot exclude additional orientational fluctuations.

Finally, the dimers were allowed to rotate about the *b* axis. Even small tilts are now found to affect drastically the calculated intensity of the observed superlattice peak with the best agreement being achieved for an anticlockwise rotation of ~1.5°. The (101) basal plane projection of the resulting structure is illustrated in Figure 3. In this configuration, the principal molecular axis lies on the (*ac*) plane and makes an angle of ~1.5° with the *c* axis; the bridging C−C bond also lies on the (*ac*) plane and is inclined at an angle of ~3.8° from the *c* axis. We also note that, consistent with the more compact, less compressible structure of azafullerene, the adopted interdimer contacts lead to a shortest C−C intermolecular distance of 3.02 Å, somewhat shorter than the equivalent one in the orientationally ordered form (space group $Pa\bar{3}$) of C_{60} (3.12 Å).

As the $C_{59}N$ monomer is isoelectronic with the singly charged C_{60}^- ion, a comparison of their structural and electronic properties is of particular interest. Unlike $(C_{59}N)_2$, which is a diamagnetic insulating solid comprising of dimers, C_{60}^- exists as a monomeric moiety in a plethora of charge-transfer salts, including the organic ferromagnet (TDAE)C_{60}.[8] In the case of the alkali-metal salts AC_{60} (A = K, Rb, Cs), the most stable form is a conducting orthorhombic phase consisting of linear chains of C_{60}^- ions formed by [2 + 2] cycloaddition reactions.[9] However, rapid quenching can also lead to the isolation of two additional metastable forms: a metallic cubic one (space group $Pa\bar{3}$), comprising of C_{60}^- monomers[10] and a nonmetallic monoclinic one (space group $C2/m$), comprising of $(C_{60})_2^{2-}$ dimers.[11] The latter is essentially isostructural with $(C_{59}N)_2$ with very similar lattice constants and a comparable center-to-center separation of 9.34 Å. Recent structural analysis[12] has shown further that the C_{60}^- units are linked by a single C−C bond in analogy with $(C_{59}N)_2$. However, while there is similarity in the structural behavior and bonding of the two dimers, calculations find that $(C_{60})_2^{2-}$ is not bound and needs the presence of the cations to be stabilized.[5]

In conclusion, synchrotron X-ray diffraction measurements indicate that solid azafullerene adopts a monoclinic structure between 278 and 500 K with strong evidence for molecular dimerization. This is consistent with both the observed diamagnetic and insulating properties of the solid and with density functional theory-based calculations which confirm the stability of the dimer.

Acknowledgment. We are grateful to the EPSRC (U.K.) for financial support and access to the synchrotron facilities at the Daresbury Laboratory and the ESRF. Partially supported by the MRL program of the National Science Foundation under award DMR-91-23048 as well as grants DMR-91-22536, DMR-91-11097, and CHE-93-00954. We thank G. Bushnell-Wye for invaluable help with the experiments.

CM960354I

---

(8) Allemand, P. M.; Khemani, K. C.; Koch, A.; Wudl, F.; Holczer, K.; Donovan, S.; Gruner, G.; Thompson, J. D. *Science* **1991**, *253*, 301. Stephens, P. W.; Cox, D.; Lauher, J. W.; Mihaly, L.; Wiley, J. B.; Allemand, P. M.; Hirsch, A.; Holczer, K.; Li, Q.; Thompson, J. D.; Wudl, F. *Nature* **1992**, *355*, 331. Lappas, A.; Prassides, K.; Vavekis, K.; Arcon, D.; Blinc, R.; Cevc, P.; Amato, A.; Feyerherm, R.; Gygax, F. N.; Schenck, A. *Science* **1995**, *267*, 1799.

(9) Stephens, P. W.; Bortel, G.; Faigel, G.; Tegze, M.; Janossy, A.; Pekker, S.; Oszlanyi, G.; Forro, L. *Nature* **1994**, *370*, 636.

(10) Lappas, A.; Kosaka, M.; Tanigaki, K.; Prassides, K. *J. Am. Chem. Soc.* **1995**, *117*, 7560.

(11) Zhu, Q.; Cox, D. E.; Fischer, J. E. *Phys. Rev. B* **1995**, *51*, 3966. Oszlanyi, G.; Bortel, G.; Faigel, G.; Tegze, M.; Granasy, L.; Pekker, S.; Stephens, P. W.; Bendele, G.; Dinnebier, R.; Mihaly, G.; Janossy, A.; Chauvet, O.; Forro, L. *Phys. Rev. B* **1995**, *51*, 12228.

(12) Oszlányi, G.; et al., personal communication.